NANO LETTERS

2007
Vol. 7, No. 7
2122−2128

Bioactive Nanofibers: Synergistic Effects of Nanotopography and Chemical Signaling on Cell Guidance

Shyam Patel,[†,‡] Kyle Kurpinski,[†,‡] Ryan Quigley,[‡] Hongfeng Gao,[§] Benjamin S. Hsiao,[||] Mu-Ming Poo,[§] and Song Li*[,†,‡]

Joint Graduate Program in Bioengineering, University of California San Francisco/ University of California Berkeley, California 94720-1762, Department of Bioengineering and Center for Tissue Bioengineering, University of California Berkeley, California 94720, Department of Molecular and Cell Biology, Helen Wills Neuroscience Institute, University of California Berkeley, California 94720, and Department of Chemistry, Stony Brook University, Stony Brook, New York 11794-3400

Received May 19, 2007

ABSTRACT

Biodegradable nanofibers have tremendous potential for tissue repair. However, the combined effects of nanofiber organization and immobilized bioactive factors on cell guidance are not well understood. In this study, we developed aligned and bioactive nanofibrous scaffolds by immobilizing extracellular matrix protein and growth factor onto nanofibers, which simulated the physical and biochemical properties of native matrix fibrils. The aligned nanofibers significantly induced neurite outgrowth and enhanced skin cell migration during wound healing compared to randomly oriented nanofibers. Furthermore, the immobilized biochemical factors (as efficient as soluble factors) synergized with aligned nanofibers to promote highly efficient neurite outgrowth but had less effect on skin cell migration. This study shed light on the relative importance of nanotopography and chemical signaling in the guidance of different cell behavior.

Native extracellular matrix (ECM) contains fibrils ranged from tens of nanometers to micrometers in scale. The organized structure of these matrix fibrils guides tissue morphogenesis and remodeling. In addition, matrix fibrils serve as "depots" for the storage of bioactive factors for the regulation of cell migration, proliferation, and differentiation. Our goal is to fabricate biodegradable and bioactive nanofibers to mimic the physical and biochemical properties of native matrix fibrils for tissue regeneration. Electrospinning technology can be used to fabricate nonwoven nanofibrous scaffolds from biological and/or synthetic polymers and has tremendous potential for tissue engineering applications.[1−4] The diameter of the individual fibers can be specifically controlled down to the nanometer range, and the fibers can be patterned through a variety of methods.[5−7] Moreover, the electrospun nanofibers have a large surface area to volume ratio, which allows for the direct attachment of ECM ligands and growth factors onto fiber surfaces to locally modulate cell and tissue function and to enhance regeneration. Although the patterning of the nanofibers has been shown to influence the alignment of cells and cellular processes,[8,9] the combined effects of patterned and bioactive nanofibers on neurite outgrowth and cell migration have not been elucidated. In this study, we fabricated aligned bioactive nanofibrous scaffolds and studied their effect on neurite outgrowth and dermal fibroblast migration to evaluate their potential for therapeutic applications.

We used biodegradable poly(L-lactide) (PLLA) (Lactel Absorbable Polymers, Pelham, AL, 1.09 dL/g inherent viscosity) to fabricate nanofibrous scaffolds by electrospinning, as described previously.[10] The PLLA solution (10% w/v in chloroform) was delivered by a programmable pump to a grounded collecting plate or mandrel in a high electric field, resulting in nanofibrous membranes or tubes. The alignment of the nanofibers was either produced during the electrospinning process (with a nonconductive portion in the middle of the collecting plate or mandrel) or postelectrospinning. To align the nanofibers postelectrospinning, the

* Corresponding author. E-mail: song_li@berkeley.edu. Telephone: (510) 665-3598. Fax: (510) 665-3599. Song Li, Ph.D., 471 Evans Hall, University of California, Berkeley, Berkeley, CA 94720.

[†] Joint Graduate Program in Bioengineering, University of California San Francisco/University of California Berkeley.

[‡] Department of Bioengineering and Center for Tissue Bioengineering, University of California Berkeley.

[§] Department of Molecular and Cell Biology, Helen Wills Neuroscience Institute, University of California Berkeley.

[||] Department of Chemistry, Stony Brook University.

10.1021/nl071182z CCC: $37.00
Published on Web 06/14/2007

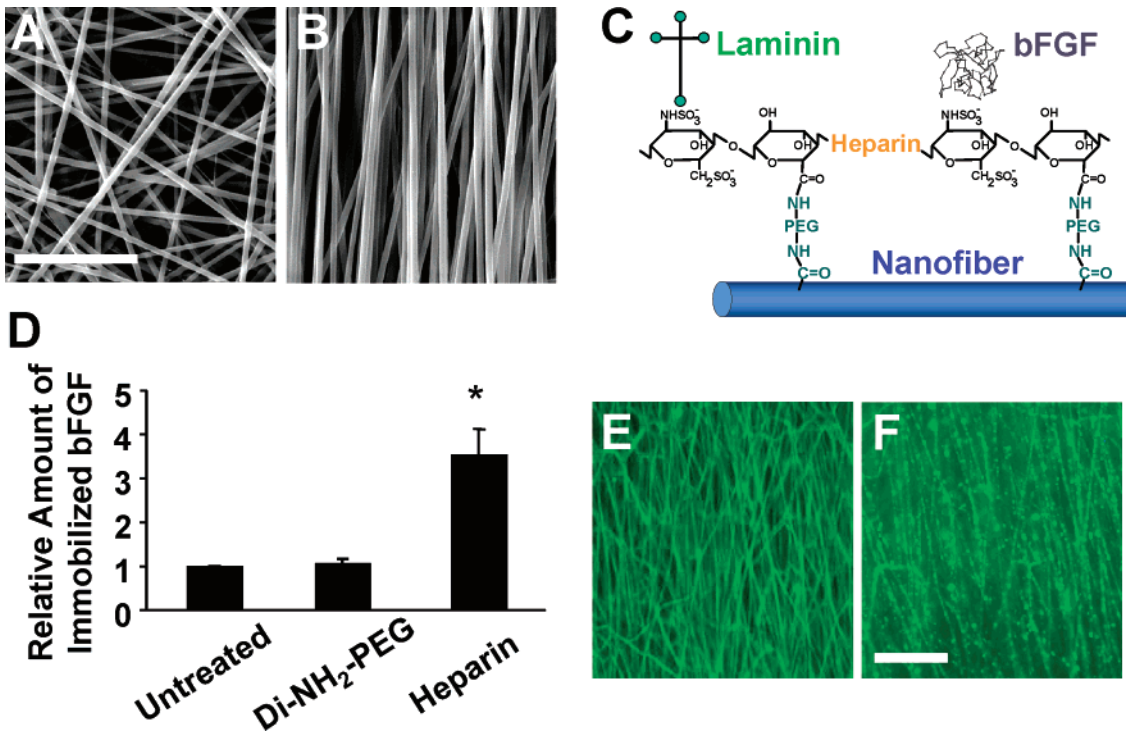

Figure 1. Characterization of aligned and bioactive nanofibers. (A) SEM image of random PLLA nanofibers. (B) SEM image of aligned PLLA nanofibers. (C) Immobilization of bFGF and laminin on PLLA nanofibers using di-NH_2-PEG and heparin as linkers. (D) Modified ELISA technique was used to show relative levels of bFGF attachment on untreated, di-NH_2-PEG-modified, and heparin-functionalized PLLA nanofibers. * $p < 0.05$ using Holm's t test (compared with the other two samples). (E) Immunostaining of immobilized laminin. (F) Immunostaining of immobilized bFGF. Scale bars = 10 μm.

electrospun scaffold was stretched uniaxially to 200% strain (which was sufficient to make aligned fibers without damaging individual fibers significantly as determined in pilot studies) at 60 °C. Nanofibrous scaffolds were approximately 100−500 μm in thickness. A piece of electrospun membrane and an electrospun tube are shown in Supporting Information Figure 1. Scanning electron microscopy (SEM) was used to visualize the organization and alignment of nanofibers (Figure 1A,B). The average nanofiber diameter was approximately 500 nm, and the length of the nanofibers was 5−10 mm in our experiments. The nanofibrous membranes with these characteristics were used in all of our experiments because pilot studies showed that nanofiber diameter between 100 and 1000 nm did not significantly affect cell alignment and neurite outgrowth.

To endow bioactivity to the surface of nanofibers, we selected an ECM protein (laminin) and a growth factor (basic fibroblast growth factor, bFGF) as representative examples. Laminin and bFGF have been shown to provide neurite extending cues to neurons[11,12] as well as growth and migration cues to dermal fibroblasts[13,14] *in vitro*. Both laminin and bFGF associate with heparin via their heparin-binding domains. Heparin has also been shown to protect bFGF from degradation and plays a key role in the bFGF cell signaling pathway.[15−17] We took advantage of these properties and developed a novel method that utilized heparin to immobilize laminin and bFGF on the surface of nanofibers while preserving their bioactivities.

We fabricated heparin-functionalized nanofibers by using di-amino-poly(ethylene glycol) (di-NH_2-PEG) as a linker molecule (Figure 1C). First, the density of reactive carboxylic groups on the PLLA nanofibers was increased by briefly treating the scaffolds with 0.01 NaOH (Sigma, St. Louis, MO). Di-NH_2-PEG (MW 3400, Sigma) molecules were then covalently attached to the carboxylic groups on the PLLA nanofibers using the zero-length cross-linkers 1-ethyl-3-(3-dimethylaminopropyl)carbodiimide hydrochloride (EDC) and *N*-hydroxysulfosuccinimide (sulfo-NHS) (Pierce Biotechnology, Rockford, IL). Heparin (Sigma) molecules were covalently attached to the free amines on the di-NH_2-PEG molecules via EDC and sulfo-NHS. Any remaining reactive sites on the nanofibrous scaffolds were blocked by incubating the samples in 10% w/v glycine in phosphate-buffered saline (PBS) solution. Then bFGF (100ng/cm^2, Peprotech, Rocky Hill, NJ) and laminin (10 μg/cm^2, Sigma) in PBS solution were incubated with the nanofibrous scaffold sequentially to allow for their binding to heparin and immobilization on the surface of nanofibers.

The attachment of bFGF and laminin molecules to heparin-functionalized PLLA nanofibers was analyzed using a modified enzyme-linked immunosorbent assay (ELISA), immunofluorescent staining, and western blotting. To compare the efficiency of different ways to immobilize bFGF, untreated, di-NH_2-PEG-modified and heparin-functionalized nanofiber membranes were incubated with bFGF in PBS. All membranes were then incubated with 1% bovine serum albumin (BSA) in PBS solution to minimize passive adsorption of antibodies. Subsequently, the samples were incubated with horseradish peroxidase (HRP)-conjugated anti-bFGF mouse monoclonal IgG antibody (R&D Systems, Min-

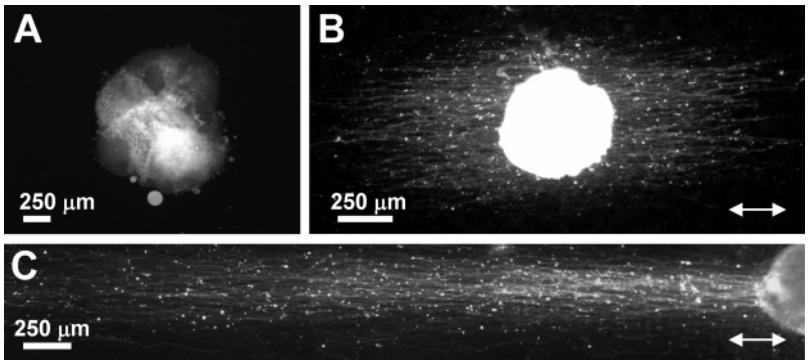

Figure 2. Neurite outgrowth from DRG tissue on nanofibers. Immunofluorescent staining of neurofilaments was used to visualize neurite outgrowth from DRG tissue on (A) untreated random nanofibers, (B) untreated aligned nanofibers, and (C) i-bFGF aligned nanofibers after 6 days of *ex vivo* culture. Scale bar = 250 μm.

neapolis, MN). The membranes were washed thoroughly, transferred to eppendorf tubes, and incubated with HRP substrate solution (hydrogen peroxide and chromagen, tetramethylbenzidine). The reaction was then stopped using 2N sulfuric acid. The absorbance of the solutions was read using a spectrophotometer (450 nm wavelength). Nonspecific adsorption of the bFGF antibody was tested on negative control samples and found to be negligible (data not shown). The results (Figure 1D) indicate that bFGF coating was significantly more efficient on nanofibers functionalized with heparin than the passive adsorption of bFGF on untreated and di-NH_2-PEG-modified nanofibers.

To visualize the uniformity of bFGF and laminin molecules on the nanofiber membranes, Immunofluorescent staining was performed. Heparin-functionalized nanofiber membranes were incubated with bFGF and/or laminin solutions in PBS. The nanofiber membranes were then immunofluorescently stained using the aforementioned primary antibodies and appropriate FITC-conjugated secondary antibodies. The fluorescent staining was visualized with a Zeiss fluorescence microscope. As shown in Figure 1E,F, laminin distributed evenly on the nanofibers while bFGF showed a spotty distribution on nanofibers, possibly due to bFGF clustering.

The attachment of bFGF and laminin onto the nanofibers was quantified using western blotting and DC protein assay, respectively. Heparin-functionalized nanofiber membranes were incubated with different concentrations of bFGF and/or laminin in PBS. The membranes were then solubilized using 4N NaOH and titrated to neutral pH using 4N HCl. The sample solutions along with various standard solutions containing known amounts of bFGF were loaded onto acrylamide gels and SDS-PAGE was performed. Western blotting was performed using a rabbit polyclonal anti-bFGF antibody (Santa Cruz Biotechnologies, Inc.). The western blot band intensities were analyzed using Scion Image to determine the amount of bFGF present on the nanofibers. An input amount of 100 ng resulted in a bound bFGF density of 13 ng/cm^2. DC protein assay (Bio-Rad, Hercules, CA) results showed that an input amount of 10 μg laminin resulted in laminin density of 4 μg/cm^2 on nanofiber surfaces. For all further studies performed herein, nanofiber scaffolds with bound bFGF density of 13 ng/cm^2 and bound laminin density of 4 μg/cm^2 were used. The immobilized laminin and bFGF were stable on the surface of nanofibers, and only ~0.1% of the immobilized proteins were released into the surrounding solution within 20 days.

To determine the effects of nanofibers on neurite outgrowth, we used an ex vivo model. In clinical situations, regeneration of severed nerves requires bridging of the two nerve stumps to facilitate outgrowth of neurites from the proximal to the distal ends and blocking the intrusion of other cell types. Currently, the most successful treatment for peripheral nerve injuries involves surgical harvesting and insertion of nerve autografts.[18] The success of the autograft is most probably due to the presence of physical and chemical cues that enhance and directly guide neurite outgrowth. This treatment method, however, requires an extra surgical procedure and often results in complications involving size mismatches, donor site morbidity, and inefficient nerve regeneration.

We postulated that a nerve guidance channel with aligned and bioactive nanofibers could facilitate and guide neurite outgrowth. To test this possibility, we harvested dorsal root ganglion (DRG) tissues from P4-P5 rats and cultured them *ex vivo* on the nanofibrous membranes. The DRG tissue was cultured in neurobasal medium supplemented with B27 and 0.5 mM L-glutamine (Invitrogen, Carlsbad, CA) for 6 days on the following aligned and random PLLA nanofiber membranes: untreated, immobilized laminin (LAM), immobilized laminin with soluble bFGF (100 ng/mL) added to the media (s-bFGF), and immobilized laminin and immobilized bFGF (i-bFGF). After 6 days of culture, neurite outgrowth from DRG tissue was analyzed by immunofluorescent staining for neurofilament-M (NFM) (using an antibody from Santa Cruz Biotechnologies, Inc.).

On untreated random nanofibers, there was no neurite outgrowth from the DRG tissue at all (Figure 2A). In contrast, neurite outgrowth from DRG tissues was observed on untreated aligned nanofibers. The neurites extended from two distinct regions of the DRG tissue and had parallel alignment to the nanofibers (Figure 2B). This bipolar extension of neurites from the DRG tissue was identical in organization to the neurite outgrowth from DRG tissue *in vivo*. These results indicate that aligned nanofibers can

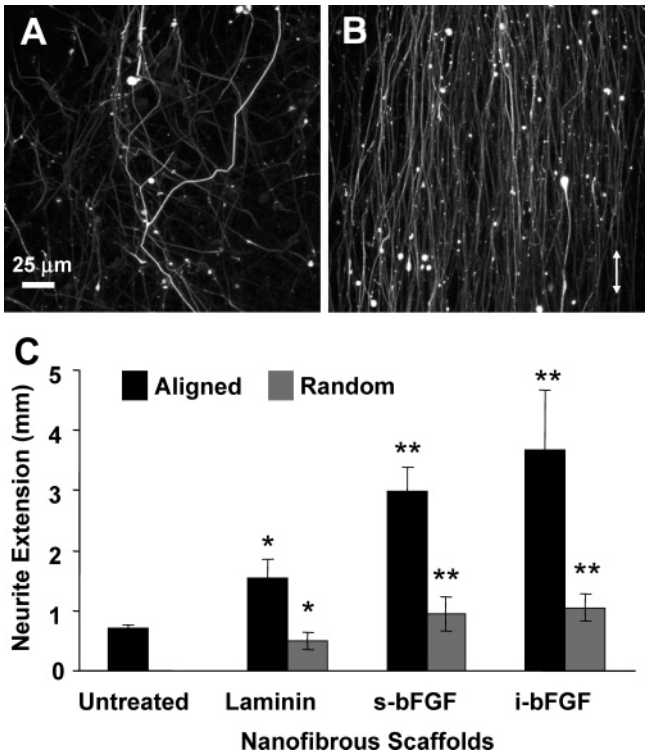

Figure 3. (A,B) High-magnification confocal microscopy images of neurite morphology on random (in A) and aligned (in B) i-bFGF PLLA nanofibers. (C) Quantitative measurement of neurite outgrowth on nanofibers from three independent experiments. All aligned samples were significantly different ($p < 0.05$ using Holm's *t* test) from their respective random samples with same chemical treatment. * Significant difference ($p < 0.05$) compared to respective (random or aligned) untreated samples. ** Significant difference ($p < 0.05$) compared to respective (random or aligned) untreated and laminin samples.

provide physical guidance and are sufficient to induce neurite outgrowth from DRG tissues.

We then determined whether biochemical cues from immobilized bFGF and/or laminin induced or enhanced neurite extension on random and aligned nanofibers. Various neurites were observed extending from DRG tissue cultured on random bioactive nanofibers coated with laminin and/or bFGF (Supporting Information Figure 2A,B). The neurites extended outward in a radial fashion from the DRG tissue and lacked uniformity in alignment. bFGF in solution (Supporting Information Figure 2C) had an effect similar to immobilized bFGF (Supporting Information Figure 2B). Neurite outgrowth from DRG tissue was significantly higher on random nanofibers with s-bFGF and i-bFGF as compared to random nanofibers with laminin alone (Supporting Information Figure 2). These results suggest that immobilized bFGF and laminin have an inductive effect on neurite outgrowth from DRG tissues. Similarly, neurite outgrowth was significantly increased on aligned nanofibers immobilized with laminin compared to untreated aligned nanofibers (Supporting Information Figure 3A). Neurite outgrowth was further enhanced by bFGF in solution (Supporting Information Figure 3B) or immobilized bFGF (Figure 2C). The longest and most dense neurite extension was observed on aligned nanofibers with s-bFGF and i-bFGF, suggesting that immobilized bFGF was as efficient as bFGF in solution. This is a great advantage because only a relatively small amount of bFGF needs to be immobilized on nanofibers and bFGF can be delivered and contained locally without systemic effects.

High-magnification confocal microscopy demonstrated that extending neurites followed the guidance of nanofibers and exhibited little to no branching on aligned nanofibers while neurites had noticeably more branching on random nanofibers (Figure 3A,B). Branching of neurites is detrimental to nerve regeneration and should be minimized.

Statistical analysis clearly showed that aligned nanofibers induced neurite outgrowth, which was synergized by immobilized laminin and bFGF (Figure 3C). The significant higher rate of neurite outgrowth on bioactive nanofibers suggest that the bioactive aligned nanofiber scaffold has tremendous potential for nerve tissue engineering by promoting and specifically directing neurite outgrowth from nerve tissue.

To determine the effects of aligned and bioactive nanofibers on skin cell migration and wound healing, we investigated the effects of nanofiber alignment and orientation as well as immobilized laminin and bFGF using an *in vitro* wound healing model, as depicted in Supporting Information Figure 4. Dermal wound healing is a complex process requiring coordination of several biological processes, including ingrowth of cells, organization of extracellular matrix, regulation of inflammation, and rapid wound coverage to prevent infection.[19] For many wounds, however, the "repair" mechanism often dominates over a more desirable "regeneration" mechanism, resulting in the formation of disorganized scar tissue instead of well-ordered skin.[20]

To examine cell migration and wound healing, normal human dermal fibroblasts (NHDFs) were seeded (in Delbecco's Modified Eagle's Medium with 10% fetal bovine serum; from Invitrogen Corp.) as monolayers on nanofibrous membranes, and a gap defect or "wound" was created across the length of the mesh. For a given sample, nanofibers were oriented in one of three ways with respect to the long axis of this wound: (1) randomly oriented, (2) aligned perpendicular to the wound axis, and (3) aligned parallel to the wound axis. Before seeding, NHDFs were stained with DiI cell tracker to determine the initial wound edges and to monitor the progression of wound coverage. NHDFs were allowed to migrate into the wound for 48 h.

Fluorescent microscopy of actin filaments revealed that NHDF migration and organization was influenced by the underlying nanofiber orientation (Figure 4A). On randomly oriented nanofibers, NHDFs migrated into the wound area and provided moderate wound coverage. However, the fibroblasts oriented randomly, similarly to the underlying randomness of the nanofibers (Supporting Information Figure 5). Conversely, on aligned nanofibers, NHDFs aligned with the direction of the fibers, and the cells were polarized to migrate under the guidance of the nanofibers (Supporting Information Figure 5). When nanofibers were oriented perpendicular to the long axis of the wound, cell migration into the wound area was greatly enhanced and the wound

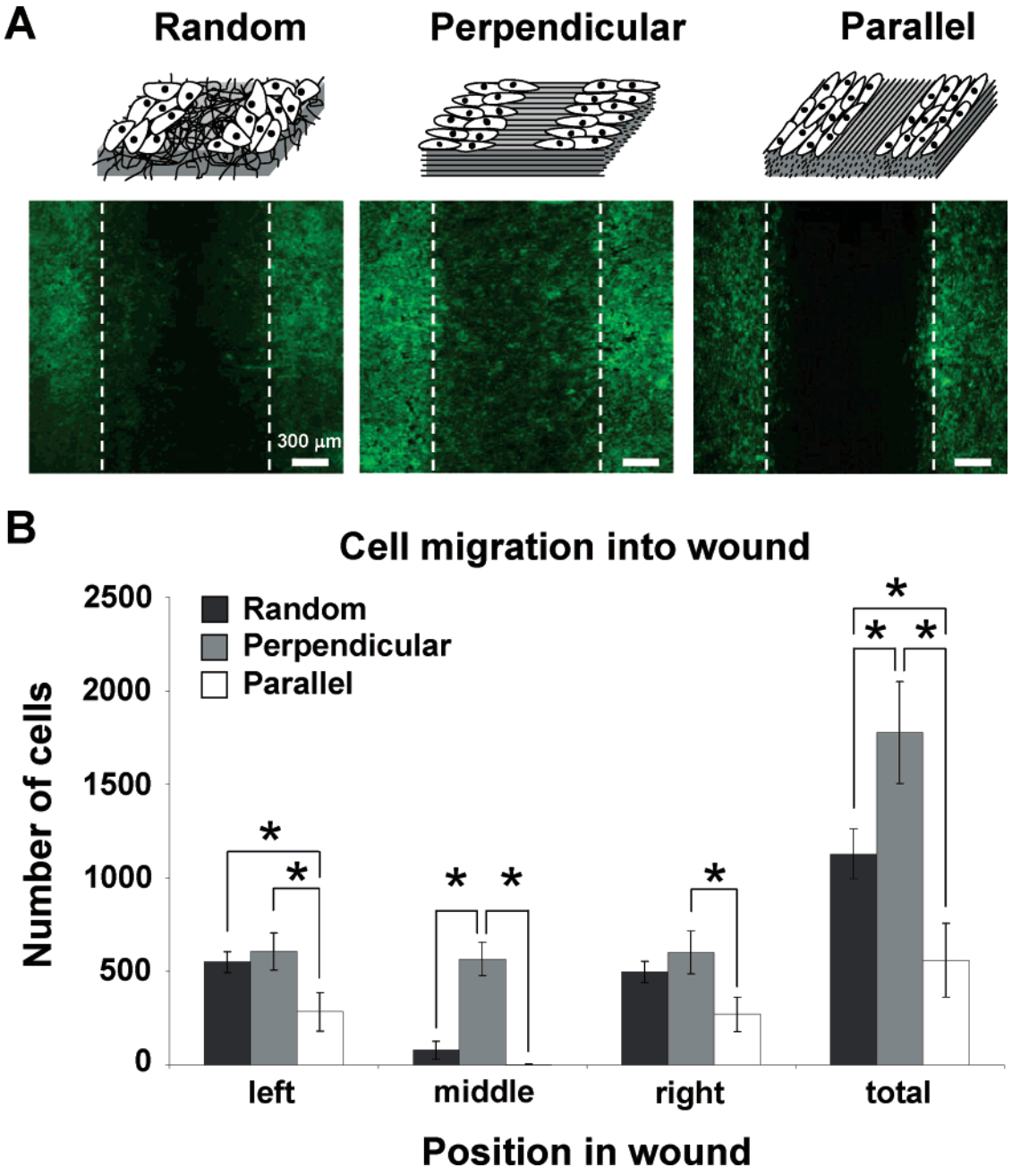

Figure 4. Nanofiber alignment and orientation enhanced cell migration into wound. (A) Dermal fibroblasts were cultured on PLLA nanofibers in an *in vitro* wound healing model. After 48 h, the cells were stained for actin filaments (green) and nuclei (blue) by using FITC phalloidin and DAPI, respectively. Dotted white lines represent initial wound edges at 0 h. Nanofibers were either random, aligned perpendicular (left to right), or aligned parallel (top to bottom) to the long edges of the wound. Scale bar is 300 μm. (B) Quantification of cells within the wound area (divided equally into left, middle, and right zones) after 48 h (from three independent experiments). *$p < 0.05$ using Holm's *t* test.

was completely covered after 2 days. However, when nanofibers were aligned parallel to the wound axis, cell migration into and coverage of the wound were severely reduced.

The number of cells migrating into the wound area was quantified based on immunofluorescent nuclear staining, and the data is displayed as a histogram in Figure 4B. The total number of fibroblasts that migrated into the wound area was significantly greater when nanofibers were aligned perpendicularly to the wound axis than when nanofibers were aligned parallel or randomly. However, when the wound area was divided into thirds, the number of cells at the sides of the wound showed no difference when comparing randomly oriented fibers to those in the perpendicular orientation. In the middle of the wound, however, only a minimal number of fibroblasts were present on random or parallel oriented nanofibers, but a significantly larger number of fibroblasts were present on perpendicularly oriented nanofibers.

To investigate the additional effects of bFGF and laminin on migration and wound coverage in our *in vitro* wound healing model, NHDFs were seeded on the following aligned nanofiber scaffolds oriented peripendicular to the wound

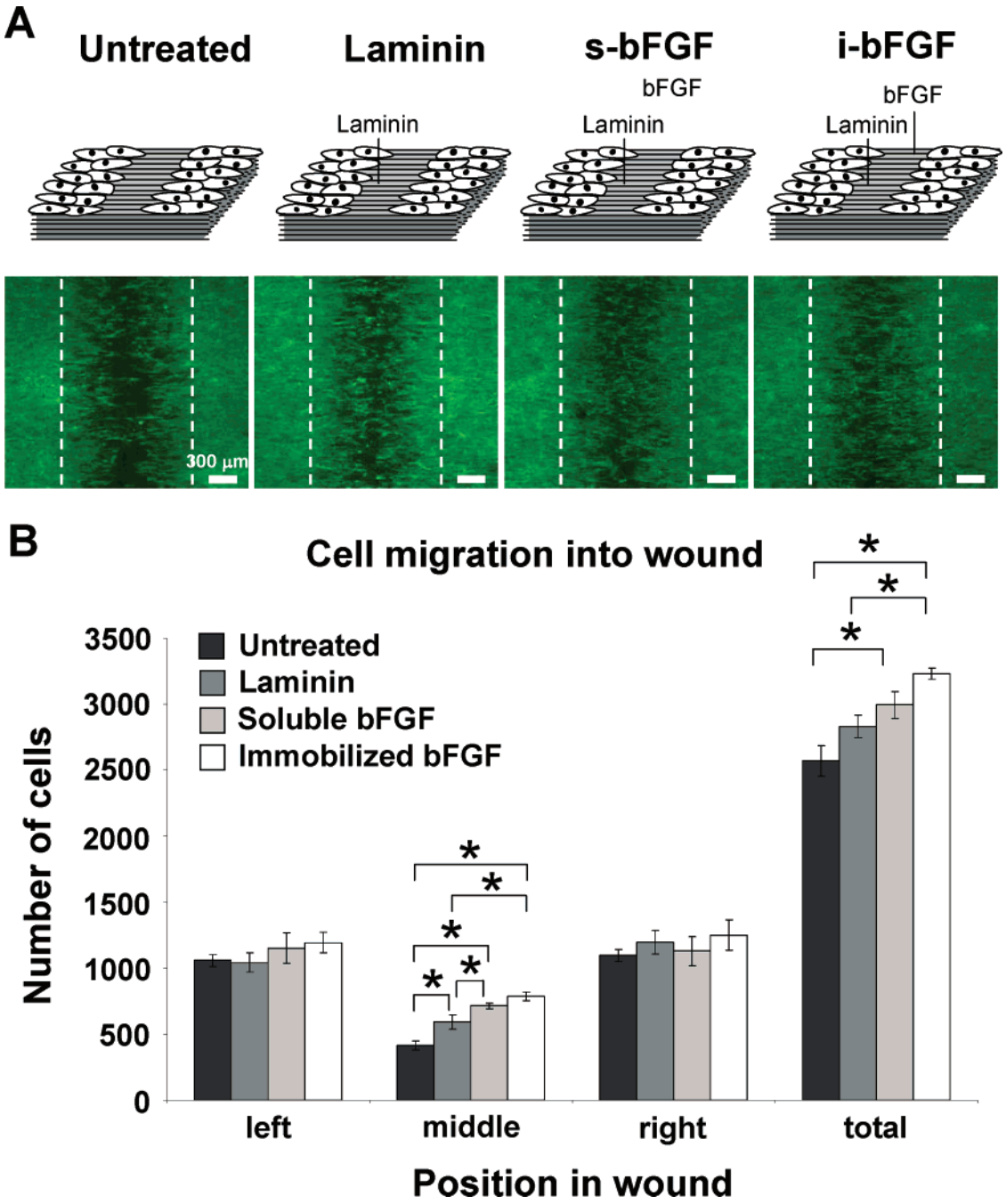

Figure 5. Chemical modification of nanofibers with bFGF enhances cell migration into wound. (A) Dermal fibroblasts were cultured on PLLA nanofibers in an *in vitro* wound healing model. In all groups, nanofibers were oriented perpendicular to the long edges of the wound and were untreated or chemically modified with laminin and/or bFGF as described. After 24 h, NHDFs were stained for whole actin (green) and nuclei (blue). Dotted white lines represent initial wound edges at 0 h. Scale bar is 300 μm. (B) Quantification of cells within the wound area after 24 h (from three independent experiments). *$p < 0.05$ using Holm's t test.

axis: untreated, LAM, s-bFGF, and i-bFGF. Because of the increased cell migration under these conditions, NHDFs were allowed to migrate into the wound for only 24 h (Figure 5A). When laminin was conjugated to the nanofibers, the wound was noticeably smaller due to enhanced cell migration. When bFGF was added in solution, this trend was increased even further, and wound coverage appeared nearly complete. Immobilized bFGF was as efficient as soluble bFGF in promoting cell migration and wound healing. Quantitative analysis (Figure 5B) showed that while there were no significant differences at the edges of the wound, the cell number in the center of the wound was significantly greater on bioactive nanofibers than on untreated nanofibers. Furthermore, both bFGF treatments resulted in a significantly greater number of fibroblasts in the wound area than the laminin treatment alone. These trends were similar when comparing the total number of cells in the wound area.

The results from this study clearly demonstrate that the nanotopographic pattern plays a critical role in neurite outgrowth and cell migration and thus the dynamic remodel-

ing of tissues. Aligned nanofibers were sufficient to induce neurite outgrowth and greatly promoted cell migration, which were further enhanced by immobilized matrix proteins and growth factors. The bioactive nanofibers make it possible to deliver and manipulate chemical cues locally in the targeting area and will improve the therapeutic efficacy without systemic side effects. The combination of nanopatterning and immobilized bioactive factors will open new avenues in tissue engineering for regenerative medicine such as nerve repair and wound healing.

How nerve tissue senses the aligned nanofibers and extends parallel neurites along the nanofibers is not clear. It is possible that the polymerization rate of neurofilaments and the signaling between axons are enhanced on aligned nanofibers. The exact mechanism awaits further investigation. Another interesting observation is that the relative importance of bioactive factors and their synergism with aligned nanofibers was different in neurite outgrowth and cell migration. Immobilized bioactive factors increased neurite outgrowth by 2−4 folds, but only enhanced cell migration by <2 folds. This could be attributed to different cellular processes (e.g., protrusion vs migration), cell types and culture conditions. In conclusion, we have shown that a bioactive, patterned nanofiber scaffold provides both physical and biochemical cues to induce, enhance, and guide neurite outgrowth and skin cell migration. The findings of this study may be used to engineer effective scaffolds for nerve and skin tissue regeneration.

Acknowledgment. This work was supported in part by Berkeley Futures Fund and grants from National Institute of Health (NS22764 to M.M.P. and HL083900 to S.L.).

Supporting Information Available: Electrospun membrane and tube with nanofibrous structure. Neurite outgrowth from DRG tissue on random nanofibers. Neurite outgrowth from DRG tissue on aligned nanofibers. Preparation of nanofiber samples for in vitro wound healing experiments. Effects of nanofiber alignment on cell orientation during wound healing. This material is available free of charge via the Internet at http://pubs.acs.org.

References

(1) Doshi, J.; Reneker, D. *J. Electrost.* **1995**, *35*, 151−160.
(2) Ma, Z.; Kotaki, M.; Inai, R.; Ramakrishna, S. *Tissue Eng.* **2005**, *11*, 101−109.
(3) Zong, X.; Kim, K.; Fang, D.; Ran. S.; Hsiao, B. S.; Chu, B. *Polymer*. **2002**, *43*, 4403−4412.
(4) Matthews, J. A.; Wnek, G. E.; Simpson, D. G.; Bowlin, G. L. *Biomacromolecules* **2002**, *3*, 232−238.
(5) Li, D.; Wang, Y. L.; Xia, Y. N. *Nano Lett.* **2003**, *3*, 1167−1171.
(6) Zong, X.; Ran, S.; Fang, D.; Hsiao, B. S.; Chu, B. *Polymer* **2003**, *44*, 4959−4967.
(7) Theron, A.; Zussman, E.; Yarin, A. L. *Nanotechnology* **2001**, *12*, 384−390.
(8) Xu, C. Y.; Inai, R.; Kotaki, M.; Ramakrishna, S. *Biomaterials* **2004**, *25*, 877−886.
(9) Yang, F.; Murugan, R.; Wang, S.; Ramakrishna, S. *Biomaterials* **2005**, *26*, 2603−2610.
(10) Huang, N. F.; Patel, S.; Thakar, R. G.; Wu, J.; Hsiao, B. S.; Chu, B.; Lee, R. J.; Li, S. *Nano Lett.* **2006**, *6*, 537−542.
(11) Manthorpe, M.; Engvall, E.; Ruoslahti, E.; Longo, F. M.; Davis, G. E.; Varon, S. *J. Cell Biol.* **1983**, *97*, 1882−1890.
(12) Rydel, R. E.; Greene, L. A. *J. Neurosci.* **1987**, *7*, 3639−3653.
(13) Grazul-Bilska, A. T.; Luthra, G.; Reynolds, L. P.; Bilski, J. J.; JOhnson, M. L.; Abdullah, S. A.; Redmer, D. A.; Abdullah, K. M. *Exp. Clin. Endocrinol. Diabetes* **2002**, *110*, 176−181.
(14) Ohgoda, O.; Sakai, A.; Koga, H.; Kanai, K.; Miyazaki, T.; Niwano, Y. *J. Dermatol. Sci.* **1998**, *17*, 123−131.
(15) Gospodarowicz, D.; Cheng, J. *J. Cell Physiol.* **1986**, *128*, 475−484.
(16) Saksela, O.; Moscatelli, D.; Sommer, A.; Rifkin, D. B. *J. Cell Biol.* **1988**, *107*, 743−751.
(17) Yayon, A.; Klagsbrun, M.; Esko, J. D.; Leder, P.; Ornitz, D. M. *Cell* **1991**, *64*, 841−848.
(18) Belkas, J. S.; Shoichet, M. S.; Midha, R. *Neurol. Res.* **2004**, *26*, 151−160.
(19) Redd, M. J.; Cooper, L.; Wood, W.; Stramer, B.; Martin, P. *Philos. Trans. R. Soc. London, Ser B* **2004**, *359* (1445), 777−84.
(20) Metcalfe, A. D.; Ferguson, M. W. *Biochem. Soc. Trans.* **2005**, *33* (Part 2), 413−417.

NL071182Z